

BIOLOGY AND RESUSPENSION IN PROWQM

by

Paul Tett⁽¹⁾, Jae-Young Lee⁽¹⁾, and Sarah Jones⁽²⁾

June 2001

| | |
|-------------------------------------|----|
| Introduction..... | 2 |
| Pelagic model..... | 2 |
| Benthic and resuspension model..... | 5 |
| Numerical methods | 6 |
| References | 7 |
| Tables..... | 9 |
| Appendix: Aggregation..... | 10 |

(1) School of Life Sciences, Napier University, 10 Colinton Road, Edinburgh EH10 5DT, U.K.email: j.lee@napier.ac.uk. (2) School of Ocean Sciences, University of Wales, Bangor LL59 5EY.

Introduction

PROWQM is a 1-D depth resolving model which couples physical and microbiological processes in the water column with sedimentation/resuspension and benthic mineralization processes, was developed during PROVESS from the earlier model COHERENS (Luyten *et al.*, 1999). This report briefly documents the water-column and benthic biological and sedimentological processes in PROVESS. It is largely draw from the model description in the paper by Lee *et al.* (ms) which includes rsimulate seasonal changes of chlorophyll, nutrients and oxygen at the PROVESS North site (59°20'N 1°00'E) in the North Sea. Figure 1* provides an overview of the relevant processes described by PROWQM.

The **pelagic biological sub-model 2MPPD** includes a 'diatomey' microplankton (MP1) and a 'flagellatey' (or microbial loop) microplankton (MP2), the cycling of silicon and nitrogen, slow sinking detritus, and fast sinking phyto-detritus. Phyto-detritus is formed by shear-driven aggregation of particulate material, using a simple algorithm for bulk processes that is derived by considering the interactions of single cells. The microplankton compartments include heterotrophic bacteria and protozoa as well as phytoplankton, and most microplankton rates are specified with the aid of a 'heterotroph fraction' parameter. The microbiological system is closed by mesozooplankton grazing pressures imposed as time varying series determined from observed zooplankton abundance. The **benthic boundary sub-model Benthos6** includes a superficial Fluff layer and a nutrient element reservoir in the consolidated sediment. Particulate material in the Fluff layer can be resuspended (in response to bed stress by near-bed flows), mineralized or carried by bioturbation into the underlying, consolidated, sediment, where it is mineralized and its nutrients returned to the water-column at rates mainly dependent on (implicit) macrobenthic pumping. Benthic denitrification can occur when mineralization rates exceed oxygen supply. The **physical and optical sub-models** of PROWQM force the biological and sedimentological processes by providing changing vertical distributions of light and shear, and bed stress. The physical sub-model solves the transport equations for all biological variables, as well as generating turbulence to bring about vertical mixing.

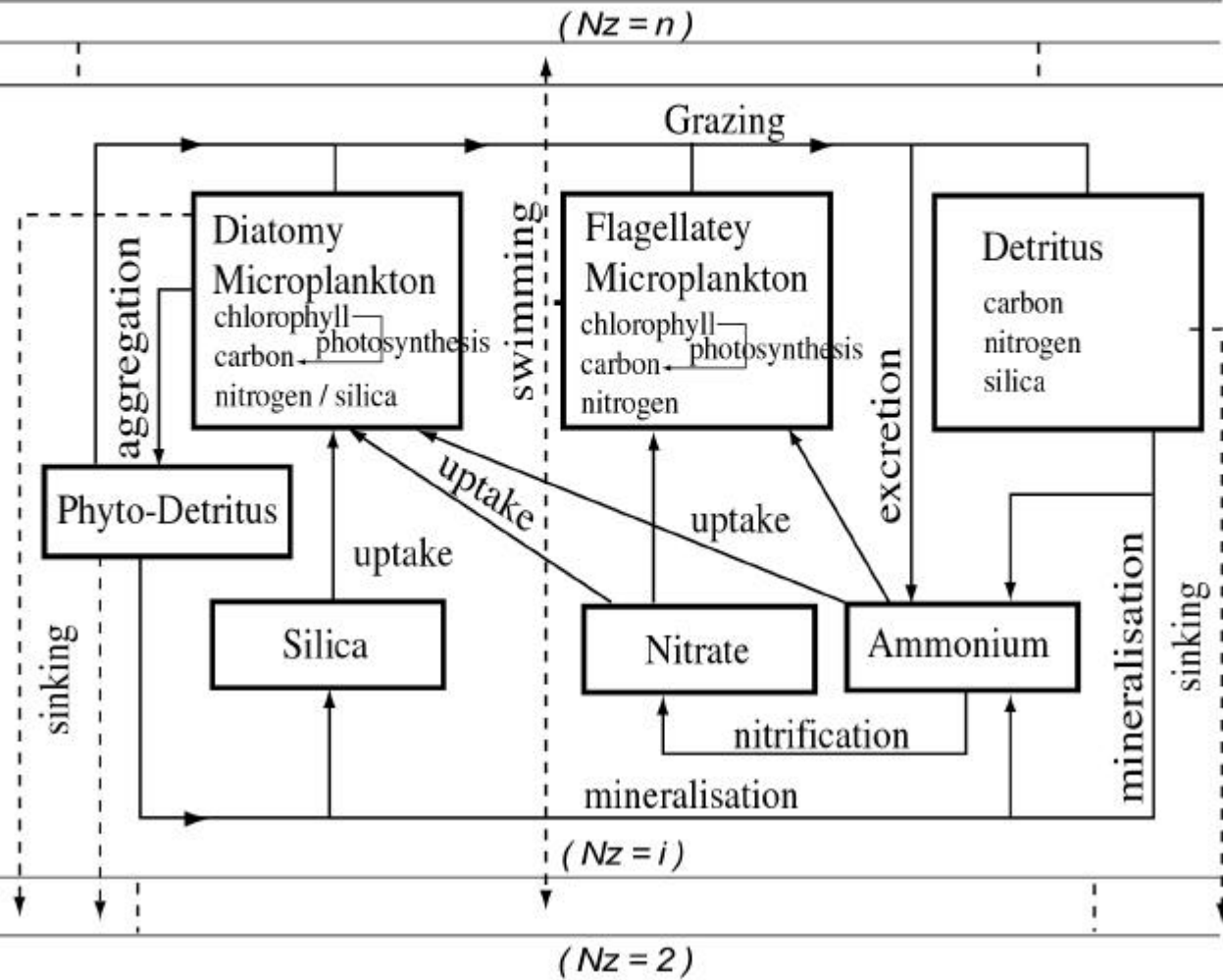
Pelagic model

2MPPD is a two-microplankton sub-model of the pelagic ecosystem excluding higher trophic levels (whose effects are represented as a grazing pressure). The sub-model includes a

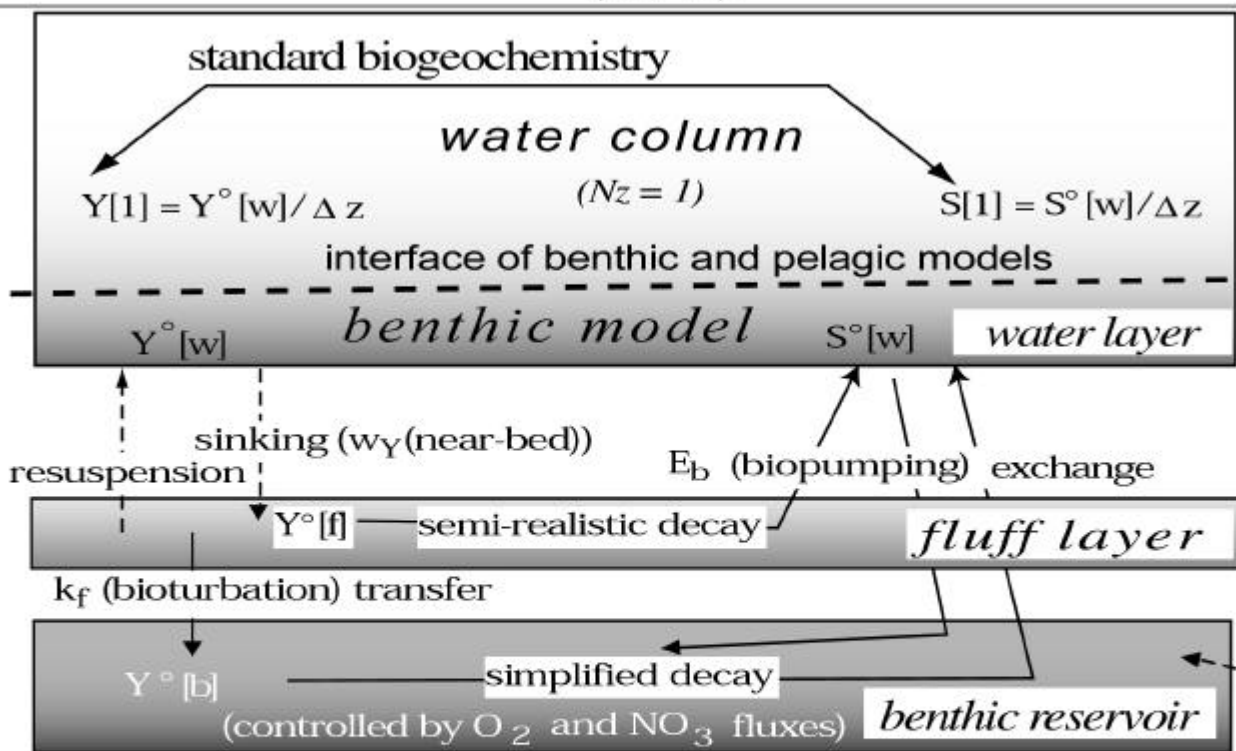
* Figure 1. The pelagic biological submodel (2MPPD, with 2 microplanktons and aggregation) and the benthic biological and resuspension submodel (Benthos6, with layers for fluff and consolidated sediment) in PROWQM.

(PROVESS) 2MPPD MODEL

(PROVESS) MP2 COMPARTMENTS



(PROVESS) LEVEL 6 BENTHIC MODEL



no explicit state variables for benthic pore water dissolved substances

'diatomey' and a 'flagellatey' microplankton, the cycling of silicon as well as nitrogen, and the formation and rapid sinking of phytodetritus as well as slower-sinking detritus. In PROWQM the evolution of a generalised tracer is described by

$$(1) \quad \frac{Y}{t} = - \frac{Y}{z} + \gamma \quad \text{concentration d}^{-1}$$

where conservative transports are described by a Fickian approximation for turbulent and advective flux:

$$(2) \quad \gamma = \langle (w + w' + w_Y) \cdot (Y + Y') \rangle - K_z \cdot \frac{Y}{z} + w_Y \cdot Y \quad \text{amount m}^{-2} \text{ d}^{-1}$$

where w_Y is a swimming or sinking velocity in the case of particulates, or zero in the case of dissolved tracers. Water advection w is taken as zero. The vertical, z , axis, increases in value from the sea-bed upwards, so positive fluxes are upwards and negative values of w_Y represent sinking. The lower boundary condition is defined by the benthic model, described below. The upper boundary condition is zero-flux for all tracers except oxygen, which has air-sea exchange parameterized following Tett & Walne (1995):

$$(3) \quad O[z=h] = -k_w \cdot W^2 \cdot (O_{\text{sat}}[z=h] - O[z=h]) \quad \text{mmol O}_2 \text{ m}^{-2} \text{ d}^{-1}$$

where W is wind speed and $O_{\text{sat}}[z=h]$ gives seawater saturation concentration at the simulated temperature of the near-surface water.

The term γ in equation (1) summarises biogeochemical sources and sinks for carbon, nitrogen, oxygen, silicon and photosynthetic pigment variables in each microplankton, detritus and water compartment. The sums of the γ -terms over all nitrogen variables, or over all silicon variables, are conservative. The terms are listed for all state variables in Table 1, and Table 2 lists rate equations. Microplankton and detritus equations for carbon, nitrogen and oxygen are essentially those of the earlier model L3VMP (Tett, 1990b; Tett & Grenz, 1994; Tett & Walne, 1995), except that there are now two types of microplankton, and the parameters for each microplankton are now defined in terms of constant autotroph and heterotroph parameters and f , the 'heterotroph fraction' of the microplankton biomass (Tett, 1998; Smith & Tett, 2000; Tett & Wilson, 2000). Autotroph and heterotroph parameter values in MP1, the diatomey microplankton, are taken as standard. The values of MP2 parameters involving cell-surface processes are increased in proportion to their relatively greater surface area. Table 3 shows the derivation of microplankton parameters from autotroph and heterotroph parameters. Table 4 focuses on the differences between MP1 and MP2. Table 5 lists detrital parameters.

2MPPD has developed from the MP component of L3VMP by adding silicon cycling and the formation of phytodetritus by shear-induced aggregation as well as by dividing the microplankton into two compartments. As an example of a γ -term, the nonconservative processes acting on MP1 carbon are described by

$$(4) \quad \gamma_{B1} = (\mu_1 - G) \cdot B_1 - k_a \cdot a_s \cdot B_1^2 \quad \text{mmol carbon m}^{-3} \text{ d}^{-1}$$

where B_1 is the biomass of this microplankton quantified as a concentration of particulate organic carbon, μ_1 is growth rate (d^{-1}) after taking account of respiratory losses, and G is grazing pressure (d^{-1}). The final group of terms gives the rate of loss due to aggregation, which converts the diatom material into phytodetritus. The expression simplifies 'coagulation kernel' theory (Jackson, 1990) for use with bulk concentrations rather than organism number concentrations (see Appendix). The parameter a_s represents 'stickiness' - the probability that an encounter between two organisms will lead to them sticking together. ϵ_s is small-scale shear, calculated from the rate of dissipation of turbulent kinetic energy given by the physical sub-model. k_a takes account of geometrical factors and unit conversions.

Microplankton growth in 2MPPD is based on a modification of the 'cell-quota, threshold limitation' model of Droop (1983):

$$(5) \quad \mu = \min(f(\langle I \rangle), f(Q), [f(SiQ)]) \quad d^{-1}$$

$$f(\langle I \rangle) = (\langle I \rangle - r_0) / (1 + r_b) \quad \text{where:} \quad \langle I \rangle = X_q N_a (Q - q_h)$$

$$f(Q) = f(Q_{min}) \cdot \mu_{max} \cdot (1 - (Q_{min}/Q)) \quad \text{where:} \quad Q = N/B$$

$$[f(SiQ) = f(SiQ_{min}) \cdot \mu_{max} \cdot (1 - (SiQ_{min}/SiQ)) \quad \text{where:} \quad SiQ = SiN/B]$$

$\langle I \rangle$ is the mean PAR experienced by microplankton at a given depth, calculated using the optical model described by Smith & Tett (2000), which takes account of self-shading by microplankton and light attenuation by other particulates. The light-controlled growth function $f(I)$ is parameterized for illumination averaged over 24 hours (Tett, 1990a). Because PROWQM includes diel variation in solar radiation, it was necessary to smooth this variation before applying it to the biological model. Both diel variability, and smoothing, are as implemented in the COHERENS model (Luyten *et al.*, 1999).

The 'cell quota', Q is the bulk ratio of cell nitrogen to cell organic carbon (or of cell silica to cell carbon in the case of diatoms and SiQ). The derivation of the microplankton equations assume that phytoplankton can take up nutrient in excess of need, so increasing their cell quota, or use stored nutrient to sustain growth when seawater supplies have been depleted. The microheterotroph component of microplankton is however assumed (Tett, 1998) to have a constant elemental composition. The silica term in equation (5) applies only to diatom microplankton.

The nitrogen quota is also important in that it controls the bulk chlorophyll:carbon ratio (see eqn. 5) and the rate of vertical movement of microplankton. Diatoms, and their associated heterotrophs, are assumed to sink more quickly when depleted of nitrogen. Phytoflagellates, accompanied by their protozoan grazers, are assumed to swim downwards when nutrient-starved and upwards when nutrient-replete.

Grazing by mesozooplankton is represented as a grazing pressure, calculated from observed biomasses of pelagic crustaceans likely to consume phytoplankton or pelagic

protozoans. The forcing time-series G is only applied when the biomass of a particular microplankton exceeds a threshold:

$$(6) \quad g_i = \begin{cases} w_g \cdot p_i \cdot G & : B_i \geq B_{i0} \\ 0 & : B_i < B_{i0} \end{cases} \quad d^{-1} \quad i = MP1 \text{ or } MP2 \text{ or phytodetritus}$$

The effect is further modified by using p_i to represent a mesozooplankton preference for a particular food and w_g for an overall weighting factor which can be adjusted to fit simulated to observed microplankton biomass. The introduction of separate thresholds for each type of food allows the simulated mesozooplankton to be switching predators, which aids model stability (Fasham *et al.*, 1990; Tett & Wilson, 2000).

Benthic and resuspension model

The Benthos6 model deals with carbon, nitrogen, oxygen and silicon. It contains three layers, representing consolidated sediment, 'fluff' and water column (Figure 2). Only particulates are represented in the sediment and fluff layers. The water column layer exists in Benthos6 only to take account of changes in solubles resulting from biogeochemical processes in the underlying layers, and to provide an interface between the benthic and pelagic models. It has no ∂ -terms of its own.

Fluff layer biogeochemical dynamics are largely those of Smith & Tett (2000) with added silica; the resuspension dynamics are modified from S. Jones *et al.* (Jones *et al.*, 1996; Jago & Jones, 1998; Jones *et al.*, 1998). For a typical particulate:

$$(7) \quad dY^o[f]/dt = w_Y \cdot Y[1] - Y[f] - k_f \cdot Y^o[f] + \partial_Y[f] \quad \text{amount } m^{-2} d^{-1}$$

where k_f is a rate (d^{-1}) of bioturbation transfer of the particulate from the fluff layer into the consolidated sediment and $Y[f]$ is the resuspension flux. $Y[1]$ is the concentration of the particulate in the model's near-bed water (at simulation gridpoint 1) and $Y^o[f]$ is the amount per square metre in the fluff layer. $\partial_Y[f]$ indicates the rate of change per square metre due to biogeochemical sources and sinks in the fluff layer.

The maximum resuspension flux is:

$$(8) \quad r^* = S \cdot (\tau / \tau_0)^n \quad g \text{ } m^{-2} \text{ } s^{-1}$$

where the bed stress τ ($kg \text{ } m^{-1} \text{ } s^{-2}$) was computed by the physical model, and related to a constant reference stress τ_0 . The resuspension coefficient S was $0.0020 \text{ } g \text{ } m^{-2} \text{ } s^{-1}$. The amount resuspended was shared between the inorganic and organic components according to their relative mass in the fluff layer (see eqn. 10). This assumes that the rate of transfer from fluff into water column is independent of particle composition and settling velocity, although the balance of resuspension and deposition varies according to the settling velocity of each component.

The Fluff layer also includes a state variable (A , g m^{-2}) representing fine inorganic particulate. The total amount of this particulate is conserved as it is resuspended and deposits, and its main roles are (i) to add mass to the contents of the Fluff layer, and (ii) to attenuate light when in suspension (Luyten *et al.*, 1999; Smith & Tett, 2000).

The remineralization model for the consolidated sediment does not evaluate solubles in pore water, because to do so would require a very short integration timestep to avoid numerical instability. Instead, it calculates the maximum oxidant flux:

$$(9) \quad \text{ox}^* = -(E/h_b) \cdot ((O[1] - O_{\min}) + (\text{NOS}[1] - \text{NOS}_{\min})) \quad \text{mmol m}^{-2} \text{ d}^{-1}$$

where h_b is the notional thickness of the consolidated sediment, and E is a temperature-dependent exchange velocity that takes into account both pore water molecular diffusion and macrobenthic pumping. $O[1]$ and $\text{NOS}[1]$ are the concentrations (mmol m^{-3}) of dissolved oxygen and nitrate in the near-bed water. O_{\min} and NOS_{\min} parameterize conditions in sediment pore water. Because the greatest potential fluxes would occur when the values of these parameters were close to zero, O_{\min} was based on the pore-water concentration of oxygen below which nitrate is used as an oxidant. NOS_{\min} was given an arbitrary low value.

All particulates bioturbated into the consolidated sediment are deemed to be converted to detritus. The actual rate of organic carbon mineralization is calculated as the minimum of temperature-dependent first-order detrital carbon decay and the mineralization supportable by ox^* . Thus the equation for sediment carbon is:

$$(10) \quad dC^{\circ}[b]/dt = k_f \cdot (B_1^{\circ}[f] + B_2^{\circ}[f] + C^{\circ}[f] + C_{pd}^{\circ}[f]) + C^{\circ}[b] \quad \text{mmol C m}^{-2} \text{ d}^{-1}$$

$$\text{where:} \quad C^{\circ}[b] = -\min\{C_{kb} \cdot f([w]), C^{\circ}[b], \text{ox}^*\}$$

If the carbon mineralization rate exceeds that supportable by the oxygen component of the oxidant flux, then denitrification takes place. Nitrogen mineralization takes place in proportion to carbon mineralization, giving rise to ammonium if the oxygen flux is completely consumed by carbon mineralization, or to nitrate if oxygen is available. Silica mineralization is a temperature dependent first-order decay. All the resulting fluxes of dissolved oxygen, nitrate, ammonium and silica impact on the water layer of the benthic model, as do the results of mineralization in the fluff layer. All temperature-dependence is described by the Arrhenius equation with a Q_{10} of 2.0, as in the pelagic model. Parameter values for the benthic model are listed in Table 6. Some of the values were obtained by fitting the model to observations at the PROVESS south site (Grenz *et al.*, inrev).

Numerical methods

PROWQM is implemented as a Fortran program using the same structure as the COHERENS program (Luyten *et al.*, 1999). Most equations in the physical sub-model are solved implicitly. In contrast, the biological and chemical terms are evaluated explicitly. Although this may

reduce the efficiency of the numerical algorithms, it has the advantage that the simulations conserve both nitrogen and silicon. The numerical scheme takes particular account of problems that might arise due to complete removal of a quantity during a timestep. In general, the pelagic and benthic models are designed to avoid such problems, but they can occur, even with a short integration timestep, in the cases of fluff layer particulates and in seawater nutrients.

Under conditions of high bed stress, particulate resuspension is controlled by the amount of particulates in the fluff layer. The numerical scheme therefore prevents the balance of resuspension and sedimentation fluxes from exceeding the amount available in the fluff or water column layers of the benthic model. For any particular constituent, the mass resuspension during a simulation timestep Δt is:

$$(11) \quad \Delta Y_i = \min \{ (r^* \cdot (Y_i^o[f] / Y^o[f]) - w_{Y_i} \cdot Y_i[1]) \cdot \Delta t, Y_i^o[f] \} \quad \text{mass m}^{-2}$$

where amounts are calculated as masses rather than as molar amounts, and $Y^o[f]$ was the total mass of particulates (including inorganics) in a square metre of the fluff layer.

In cell quota models, nutrient uptake is a highly effective process that can result in very low simulated concentrations of ambient nutrient. The numerical scheme thus has to prevent the uptake of nutrient during a timestep from exceeding the amount available at the start of the timestep. We found that, in some cases, all available nutrient was captured by the microplankton which was simulated first in each time-step. Thus the numerical scheme includes random alternation of the order of calculation, so that MP1 and MP2 had an equal probability of obtaining scarce nutrient.

References

- Droop, M. R. (1983). 25 years of algal growth kinetics - a personal view. *Botanica Marina*, 26, 99-112.
- Fasham, M. J. R., Ducklow, H. W. & McKelvie, S. M. (1990). A nitrogen-based model of plankton dynamics in the oceanic mixed layer. *Journal of Marine Research*, 48, 591-639.
- Grenz, C., Harris, P., E. Alliot, Denis, L., K., J., Harvey, S. M., Ezzi, I., *et al.* (ms). Benthic and near bed fluxes of oxygen and nutrients in Southern North Sea : short term variability related to tidal cycles. *Journal of Sea Research*, submitted.
- Jackson, G. A. (1990). A model of the formation of marine algal flocs by physical coagulation processes. *Deep-Sea Research*, 37, 1197-1211.
- Jackson, G. A. (2001). Effect of coagulation on a model planktonic food web. *Deep Sea Research I*, 48, 95-123.
- Jackson, G. A., Maffione, R., Costello, D. K., Alldredge, A. L., Logan, B. E. & Dam, H. G. (1997). Particle size spectra between 1 μm and 1 cm at Monterey Bay determined using multiple instruments. *Deep-Sea Research I*, 44, 1739-1767.
- Jago, C. F. & Jones, S. E. (1998). Observation and modelling of the dynamics of benthic fluff resuspended from a sandy bed in the southern North Sea. *Continental Shelf Research*, 18, 1255-1282.

- Jones, S. E., Jago, C. F., Bale, A. J., Chapman, D., Howand, R. & Jackson, J. (1998). Aggregation and resuspension of suspended particulate matter at a seasonally stratified site in the southern North Sea: physical and biological controls. *Continental Shelf Research*, 18, 1283-1309.
- Jones, S. E., Jago, C. F. & Simpson, J. H. (1996). Modelling suspended sediment dynamics in tidally stirred and periodically stratified waters: progress and pitfalls. Mixing Process in Estuaries and Coastal Seas, ed. Patriarchi, C. B., American Geophysical Union, Coastal and Estuarine Studies, Vol.44: 315-338.
- Lee, J.-Y., Tett, P., Jones, K., Jones, S., Luyten, P., Smith, C. & Wild-Allen, K. (ms). The PROWQM physical-biological model with benthic-pelagic coupling applied to the northern North Sea. *Journal of Sea Research*, submitted.
- Luyten, P. J., Jones, J. E., Proctor, R., Tabor, A., Tett, P. & Wild-Allen, K. (1999). COHERENS - a coupled hydrodynamical-ecological model for regional and shelf seas: user documentation. Management Unit of the Mathematical Models of the North Sea, MUMM Internal Document, 911pp.
- Pruppacher, H. R. & Klett, J. D. (1980). Microphysics of Clouds and Precipitation. D. Riedel Publishing Co., Boston.
- Smith, C. L. & Tett, P. (2000). A depth resolving numerical model of physically forced microbiology at the European shelf edge. *Journal of Marine Systems*, 26, 1-36.
- Tett, P. (1990a). The Photic Zone. Light and Life in the Sea, ed. Herring, P. J., Campbell, A. K., Whitfield, M. & Maddock, L., Cambridge University Press, Cambridge, U.K., 59-87.
- Tett, P. (1990b). A three layer vertical and microbiological processes model for shelf seas. *Proudman Oceanographic Laboratory*, 14, 85pp.
- Tett, P. (1998). Parameterising a microplankton model. Napier University, Edinburgh, Report.
- Tett, P. & Grenz, C. (1994). Designing a simple microbiological-physical model for a coastal embayment. *Vie et Milieu*, 44, 39-58.
- Tett, P. & Walne, A. (1995). Observations and simulations of hydrography, nutrients and plankton in the southern North Sea. *Ophelia*, 42, 371-416.
- Tett, P. & Wilson, H. (2000). From biogeochemical to ecological models of marine microplankton. *Journal of Marine Systems*, 25, 431-446.

Tables

1. State variables and -terms in 2MPPD.
2. (Pelagic) rate equations.
3. Microplankton parameters.
4. Differences between the microplanktons.
5. Detrital and other pelagic biogeochemical parameters.
6. Benthic sub-model.

Table 1: State Variables and β -terms in 2MPPD

| Symbol | State Variable | β -term | processes |
|-------------------|--|--|--|
| B ₁ | MP1 carbon (mmol C m ⁻³) | $B_1 = (\mu_1 - g_1) \cdot B_1 - k_a \cdot a_s \cdot s \cdot B_1^2$ | growth, grazing, aggregation |
| B ₂ | MP2 carbon (mmol C m ⁻³) | $B_2 = (\mu_2 - g_2) \cdot B_2$ | growth, grazing |
| C | detrital carbon (mmol C m ⁻³) | $C = (1 - \gamma) \cdot (g_1 \cdot B_1 + g_2 \cdot B_2 + g_{pd} \cdot C_{pd}) - C_r \cdot C$ | defecation, respiration |
| C _{pd} | phytodetrital carbon (mmol C m ⁻³) | $C_{pd} = k_a \cdot a_s \cdot s \cdot B_1^2 - g_{pd} \cdot C_{pd} - r_{pd} \cdot C_{pd}$ | aggregation, grazing, resp. |
| M | detrital nitrogen (mmol N m ⁻³) | $M = (1 - \gamma) \cdot (g_1 \cdot N_1 + g_2 \cdot N_2 + g_{pd} \cdot M_{pd}) - M_r \cdot M$ | defecation, NH ₄ ⁺ release |
| M _{pd} | phytodetrital N (mmol N m ⁻³) | $M_{pd} = Q_1 \cdot k_a \cdot a_s \cdot s \cdot B_1^2 - g_{pd} \cdot M_{pd} - N_{r_{pd}} \cdot M_{pd}$ | aggregation, grazing, NH ₄ ⁺ |
| N ₁ | MP1 nitrogen (mmol N m ⁻³) | $N_1 = u_1 \cdot B_1 - g_1 \cdot N_1 - Q_1 \cdot k_a \cdot a_s \cdot s \cdot B_1^2$ | uptake, grazing, aggregation |
| N ₂ | MP2 nitrogen (mmol N m ⁻³) | $N_2 = u_2 \cdot B_2 - g_2 \cdot N_2$ | uptake, grazing |
| SiN ₁ | MP1 silica (mmol Si m ⁻³) | $SiN_1 = Siu_1 \cdot B_1 - g_1 \cdot SiN_1 - SiQ_1 \cdot k_a \cdot a_s \cdot s \cdot B_1^2$ | uptake, grazing, aggregation |
| SiM | detrital silica (mmol Si m ⁻³) | $SiM = (1 - \gamma) \cdot (g_1 \cdot SiN_1 + g_{pd} \cdot SiM_{pd}) - Si_r \cdot SiM$ | defecation, mineralization |
| SiM _{pd} | phytodetrital silica (mmol Si m ⁻³) | $SiM_{pd} = SiQ_1 \cdot k_a \cdot a_s \cdot s \cdot B_1^2 - (g_{pd} + Si_{r_{pd}}) \cdot SiM_{pd}$ | aggregation, grazing, mineraliz. |
| O | dissolved oxygen (mmol O ₂ m ⁻³) | $O = O_q \cdot B \cdot (\mu_1 \cdot B_1 + \mu_2 \cdot B_2 - r_C \cdot C) - O_q \cdot N \cdot NH_r \cdot NHS$ | (net) growth, resp., nitrification |
| NHS | dissolved ammonium (mmol N m ⁻³) | $NHS = -(NH_{u_1} \cdot B_1 + NH_{u_2} \cdot B_2) + (r_M \cdot M + N_{r_{pd}} \cdot M_{pd}) - NH_r \cdot NHS + (1 - e) \cdot \gamma \cdot (g_1 \cdot N_1 + g_2 \cdot N_2 + g_{pd} \cdot M_{pd})$ | uptake, mineralization, nitrification, excretion |
| NOS | dissolved oxidised N (mmol N m ⁻³) | $NOS = -(NO_{u_1} \cdot B_1 + NO_{u_2} \cdot B_2) + NH_r \cdot NHS$ | uptake, nitrification |
| SiS | dissolved silica (mmol Si m ⁻³) | $SiS = -Si_{u_1} \cdot B_1 - Si_{r_M} \cdot SiM - Si_{r_{pd}} \cdot SiM_{pd}$ | uptake, mineralisation |
| NZ | mesozooplankton N (mmol N m ⁻³) | $NZ = (1 - e) \cdot \gamma \cdot (g_1 \cdot N_1 + g_2 \cdot N_2 + g_{pd} \cdot M_{pd})$ | grazing |
| | derived variable | equation | units or process |
| Q | microplankton cell quota | $Q_i = N_i / B_i$ (i=1 for MP1, i=2 for MP2) $SiQ_1 = SiN_1 / B_1$ | mmol nutrient (mmol C) ⁻¹ |
| X ₁ | diatom chlorophyll | $X_1 = X_q \cdot N_a \cdot (Q_1 - q_h \cdot 1) \cdot B_1$ | mg m ⁻³ |
| X ₂ | flagellate m ⁻³ | $X_2 = X_q \cdot N_a \cdot (Q_2 - q_h \cdot 2) \cdot B_2$ | mg m ⁻³ |
| X _{pd} | mg phytodetrital chlorophyll m ⁻³ | $X_{pd} = X_q \cdot N_a \cdot (Q_1 - q_h \cdot 1) \cdot k_a \cdot a_s \cdot s \cdot B_1^2 - g_{pd} \cdot X_{pd} - X_{r_{pd}} \cdot X_{pd}$ | aggregation, grazing, decay |

Table 2: (Pelagic) Rate Equations

| Rate variable | Equation | units |
|---|--|--|
| microplankton growth rate [silica control only in MP1] | $\mu = \min(f(<I>), f(Q), [f(\text{Si}Q)])$ $f(I) = (<I> - r_0)/(1 + r_b) \text{ where: } = X_q N_a \cdot (Q - q_h)$ $f(Q) = f(\text{Si}Q) \cdot \mu_{\max} \cdot (1 - (Q_{\min}/Q))$ $[f(\text{Si}Q) = f(\text{Si}Q_{\min}) \cdot \mu_{\max} \cdot (1 - (\text{Si}Q_{\min}/\text{Si}Q))]$ | d ⁻¹ |
| microplankton nitrogen uptake | $\text{NO}_u = f(\text{NO}) \cdot \text{NO}_{u\max} \cdot f(\text{NOS}) \cdot f_{\text{in}}(\text{NHS}) \cdot f_{\text{in1}}(Q)$ $\text{NH}_u = f(\text{NH}_4) \cdot \text{NH}_{u\max} \cdot f(\text{NHS}) \cdot f_{\text{in2}}(Q)$ $f(\text{NOS}) = \text{NOS}/(k_{\text{NOS}} + \text{NOS})$ $f(\text{NHS}) = \frac{\text{NHS}/(k_{\text{NHS}} + \text{NHS})}{1} : Q \leq Q_{\max}$ $: Q > Q_{\max}$ $f_{\text{in}}(\text{NHS}) = 1/(1 + (\text{NHS}/k_{\text{in}}))$ $f_{\text{in1}}(Q) = \frac{(1 - ((Q - q_h)/(Q_{\max} - q_h)))}{0} : Q \leq Q_{\max}$ $: Q > Q_{\max}$ $f_{\text{in2}}(Q) = 1 - ((Q - q_h)/(Q_{\max} - q_h))$ | mmol N (mmol C) ⁻¹ d ⁻¹ |
| MP1 silica uptake | $\text{Si}_{u1} = f(\text{Si}) \cdot \text{Si}_{u\max} \cdot f(\text{Si}S) \cdot f_{\text{in}}(\text{Si}Q)$ $f(\text{Si}S) = \frac{\text{Si}S/(k_{\text{Si}S} + \text{Si}S)}{1} : \text{Si}Q \leq \text{Si}Q_{\max}$ $: \text{Si}Q > \text{Si}Q_{\max}$ $f_{\text{in2}}(\text{Si}Q) = 1 - ((\text{Si}Q - \text{Si}q_h)/(\text{Si}Q_{\max} - \text{Si}q_h))$ | mmol SiO ₂ (mmol C) ⁻¹ d ⁻¹ |
| detrital respiration rate (phytodetrital rate similar) | $C_r = f(O) \cdot C_{r\max} \cdot (O/(k_O + O)) \cdot f(MQ)$ $f(MQ) = \frac{(1 - (MQ_{\min}/(M/C)))^2}{0} : MQ > MQ_{\min}$ $: MQ \leq MQ_{\min}$ <p>where: $MQ = M/C$</p> | d ⁻¹ |
| detrital ammonium release rate | $M_r = f(O) \cdot M_{r\max} \cdot f(MQ)$ <p align="center">(phytodetrital rate similar)</p> | d ⁻¹ |
| nitrification rate | $\text{NH}_r = f(\text{NH}_4) \cdot \text{NH}_{r\max} \cdot (O/(\text{NH}_4 k_O + O))$ | d ⁻¹ |
| detrital silica release rate (phytodetrital rate similar) | $\text{Si}_r = f(\text{Si}Q_d) \cdot \text{Si}_{r\max}$ $f(\text{Si}Q_d) = \frac{\text{Si}_{r\max}}{0} : \text{Si}Q_d > \text{Si}Q_{\text{mind}}$ $: \text{Si}Q_d \leq \text{Si}Q_{\text{mind}}$ <p>where: $\text{Si}Q_d = \text{Si}M/C$</p> | d ⁻¹ |
| grazing pressure | $g_i = \frac{w_g \cdot p_i \cdot G}{0} : B_i \geq B_{i0}$ $: B_i < B_{i0} \text{ for } i = \text{MP1, MP2, pd}$ | d ⁻¹ |
| temperature effect | $f(T) = \exp((T - T_{\text{ref}}) \cdot k) \quad T_{\text{ref}} = 20^\circ\text{C}, k = 0.07^\circ\text{C}^{-1}$ | (ratio) |

Table 3: Microplankton parameters
(a) standard derived parameters

| Parameter | Derivation | units |
|--|---|---|
| photosynthetic efficiency | $= k \cdot \frac{r_0}{\mu}$ $k = 0.0864 \text{ s d}^{-1} \text{ nmol mmol}^{-1} \times 4.15 \text{ } \mu\text{E J}^{-1}$ | mmol C (mg chl) ⁻¹ d ⁻¹ (W m ⁻²) ⁻¹ |
| basal respiration rate | $r_0 = (r_{0a} \cdot (1 - \frac{r_1}{r_i}) + r_{0h} \cdot (1 + b_a)) \cdot (r_1/r_i)$ | d ⁻¹ |
| respiration slope | $b = \frac{b_a \cdot (1 + b_h \cdot \frac{r_1}{r_i}) + b_h}{0} : \mu > 0$ $0 : \mu = 0$ | (ratio) |
| max. nutrient-controlled growth rate* | $\mu_{\max} = \mu_{\max a} \cdot (1 - \frac{r_1}{r_i}) / (1.2 - \frac{r_1}{r_i})$ | d ⁻¹ |
| minimum N quota | $Q_{\min} = Q_{\min a} \cdot (1 - \frac{r_1}{r_i}) + q_h$ | mmol N (mmol C) ⁻¹ |
| maximum N quota | $Q_{\max} = Q_{\max a} \cdot (1 - \frac{r_1}{r_i}) + q_h$ | mmol N (mmol C) ⁻¹ |
| max. NO ₃ ⁻ uptake rate* | $\text{NO}_{u\max} = \text{NO}_{u\max a} \cdot (1 - \frac{r_1}{r_i}) \cdot (r_1/r_i)$ | mmol N (mmol C) ⁻¹ d ⁻¹ |
| max. NH ₄ ⁺ uptake rate* | $\text{NH}_{u\max} = \text{NH}_{u\max a} \cdot (1 - \frac{r_1}{r_i}) \cdot (r_1/r_i)$ | mmol N (mmol C) ⁻¹ d ⁻¹ |

(b) standard autotroph parameters

| Symbol | Description | Value | units |
|-----------------------|---|-------|---|
| | phytoplankton photosynthetic pigment attenuation cross-section for mean submarine PAR | 0.035 | m ² (mg chl) ⁻¹ |
| | quantum yield of photosynthesis | 40 | nmol C μE^{-1} |
| r_{0a} | phytoplankton basal respiration rate | 0.03 | d ⁻¹ |
| b_a | slope of phytoplankton respiration on growth | 0.5 | (ratio) |
| X_{qN_a} | yield of chlorophyll from nitrogen assimilated by phytoplankton | 2.0 | mg chl (mmol N) ⁻¹ |
| $\mu_{\max a}$ | maximum nutrient-controlled growth rate, at 20°C | 3.0 | d ⁻¹ |
| $\text{NO}_{u\max a}$ | maximum nitrate uptake rate, at 20°C | 0.5 | mmol N (mmol C) ⁻¹ d ⁻¹ |
| $\text{NH}_{u\max a}$ | maximum ammonium uptake rate, at 20°C | 1.5 | mmol N (mmol C) ⁻¹ d ⁻¹ |
| k_{NHS} | ammonium conc. at which uptake is half max. | 0.24 | mmol NH ₄ ⁺ m ⁻³ |
| k_{NOS} | nitrate conc. at which uptake is half max. | 0.32 | mmol NO ₃ ⁻ m ⁻³ |
| k_{in} | NH ₄ ⁺ conc. at which nitrate uptake is half max. | 0.5 | mmol NH ₄ ⁺ m ⁻³ |
| $Q_{\min a}$ | minimum cell nitrogen content | 0.05 | mmol N (mmol C) ⁻¹ |
| $Q_{\max a}$ | maximum cell nitrogen content | 0.20 | mmol N (mmol C) ⁻¹ |

(c) standard heterotroph parameters

| Symbol | Description | Value | units |
|----------|---|-------|-------------------------------|
| r_{0h} | microheterotroph basal respiration rate | 0.02 | d ⁻¹ |
| b_h | slope of microheterotroph respiration on growth | 1.5 | (ratio) |
| q_h | constant microheterotroph cell nitrogen content | 0.18 | mmol N (mmol C) ⁻¹ |

Table 4: Differences between the microplanktons

| | | MP1 (i=1) | MP2 (i=2) | units |
|------------------------------------|---|-----------------------------------|-----------------------|---|
| | dominant autotroph | diatoms | flagellates | |
| | heterotrophs | spring ciliates & dinoflagellates | summer microbial loop | |
| assigned values | | | | |
| r | notional size (spherical radius) | 5 | 1.5 | μm |
| | heterotroph fraction | 0.125 | 0.60 | (ratio) |
| main microplankton model | | derived | values | (see Table 3) |
| μ _{max} | maximum growth rate (at 20°C) | 2.442 | 2.00 | d ⁻¹ |
| u _{max} | max. nutrient uptake rate (NH ₄ ⁺) (20°C) (NO ₃ ⁻) | 1.313 0.438 | 2.00 0.667 | mmol (mmol C) ⁻¹ d ⁻¹ |
| Q _{min} | minimum nitrogen quota | 0.066 | 0.128 | mmol N (mmol C) ⁻¹ |
| Q _{max} | maximum nitrogen quota | 0.198 | 0.188 | mmol N (mmol C) ⁻¹ |
| | (max.) photosynthetic efficiency | 0.502 | 0.502 | mmol C (mg chl) ⁻¹ d ⁻¹ (W m ⁻²) ⁻¹ |
| (max.) | chlorophyll: carbon ratio at Q _{max} | 0.35 | 0.16 | mg chl (mmol C) ⁻¹ |
| r ₀ | basal respiration rate | 0.030 | 0.100 | d ⁻¹ |
| r _b | respiration increase with growth | 0.781 | 1.850 | (ratio) |
| assigned silicon parameters | | | | |
| Si u _{maxa} | max.algal silica uptake rate (20°C) | 0.40 | | mmol Si (mmol C) ⁻¹ d ⁻¹ |
| k _{SiS} | silica conc. for half max. uptake | 0.32 | | mmol S m ⁻³ |
| Si Q _{mina} | minimum diatom silica content | 0.050 | | mmol Si (mmol C) ⁻¹ |
| Si Q _{maxa} | maximum diatom silica content | 0.12 | | mmol Si (mmol C) ⁻¹ |
| Si q _h | microheterotroph silica content | 0.0 | | mmol Si (mmol C) ⁻¹ |
| microplankton model derived | | values for | silicon | (see Table 3) |
| Si u _{max} | maximum silica uptake rate (20°C) | 0.35 | | mmol Si (mmol C) ⁻¹ d ⁻¹ |
| Si Q _{min} | min. microplankton silica content | 0.044 | | mmol Si (mmol C) ⁻¹ |
| Si Q _{max} | max. microplankton silica content | 0.105 | | mmol Si (mmol C) ⁻¹ |
| other values | | | | |
| p | mesozooplankton grazing pref. | 1.0 | 1.0 | (ratio) |
| B ₀ | minimum biomass for mzp grazing | 0.42 | 0.42 | mmol C m ⁻³ |
| w _{Bmax} | maximum sinking/swimming rate | -5.0 | +2.0 | m d ⁻¹ |
| w _{Bmin} | minimum sinking/swimming rate | -0.5 | | m d ⁻¹ |

vertical movement equations

| | | |
|-------------------|---|-------------------|
| MP1 sinking rate | $w_{B1} = ((Q_1 - Q_{min1}) / (Q_{max1} - Q_{min1})) \cdot (w_{Bmin1} - w_{Bmax1}) + w_{Bmax1}$ | m d ⁻¹ |
| MP2 swimming rate | $w_{B2} = 2 \cdot ((Q_2 - Q_{mean2}) / (Q_{max2} - Q_{min2})) \cdot w_{Bmax2}$ $Q_{mean2} = (Q_{max2} + Q_{min2}) / 2$ | m d ⁻¹ |

Table 5: Detrital and other pelagic biogeochemical parameters

| Symbol | Description | Value | Units |
|--------------------|--|-------------------|--|
| | mesozooplankton assimilation efficiency | 0.6 | (ratio) |
| e | mesozooplankton nitrogen excretion fraction | 0.5 | (ratio) |
| $C_{r_{\max}}$ | detrital carbon maximum mineralisation rate (at 20°C) | 0.06 | d ⁻¹ |
| $M_{r_{\max}}$ | detrital nitrogen maximum mineralisation rate (at 20°C) | 0.08 | d ⁻¹ |
| $Si_{r_{\max}}$ | detrital silica maximum mineralisation rate (at 20°C) | 0.02 | d ⁻¹ |
| $M_{Q_{\min}}$ | detrital minimum nitrogen content | 0.09 | mmol N (mmol C) ⁻¹ |
| $Si_{Q_{\min d}}$ | detrital minimum silicon content | 0.09 | mmol Si (mmol C) ⁻¹ |
| k_O | O ₂ half-saturation conc. for detrital C mineralisation | 10 | mmol O ₂ m ⁻³ |
| $C_{r_{\max pd}}$ | phytodeutral carbon max. mineralisation rate (at 20°C) | 0.08 | d ⁻¹ |
| $M_{r_{\max pd}}$ | phytodeutral nitrogen max. mineralisation rate (20°C) | 0.06 | d ⁻¹ |
| $Si_{r_{\max pd}}$ | phytodeutral silica max. mineralisation rate (at 20°C) | 0.02 | d ⁻¹ |
| $M_{Q_{\min pd}}$ | phytodeutral minimum nitrogen content | 0.09 | mmol N (mmol C) ⁻¹ |
| $Si_{Q_{\min pd}}$ | phytodeutral minimum silicon content | 0.09 | mmol Si (mmol C) ⁻¹ |
| $NH_{r_{\max}}$ | max. nitrification (ammonium-oxidation) rate (20°C) | 0.1 | d ⁻¹ |
| NH_{k_0} | oxygen conc. at which nitrification is half-max. | 30 | mmol O ₂ m ⁻³ |
| O_{qB} | oxygen change associated with carbon biomass change | 1.0 | mmol O ₂ (mmol C) ⁻¹ |
| O_{qN} | oxygen change associated with NO ₃ ⁻ <--> NH ₄ ⁺ | 2.0 | mmol O ₂ (mmol N) ⁻¹ |
| k_a | diatom microplankton aggregation factor, taking into account geometry and cell carbon content* | 0.0215 - 0.215 | m ³ (mmol C) ⁻¹ s d ⁻¹ |
| a_s | diatom microplankton stickiness* | 0.25 - 1.0 | (ratio) |
| w_C | vertical movement (sinking) rate of detritus | -5.0 | m d ⁻¹ |
| w_{Cpd} | vertical movement (sinking) rate of phytodetritus | -100.0 | m d ⁻¹ |

Table 6. Benthic sub-model
(a) consolidated sediment state variable equations

| state variable | equation | units |
|--------------------------------------|---|---|
| (detrital) carbon, $C^{\circ}[b]$ | $dC^{\circ}[b]/dt = k_f.(B_1^{\circ}[f]+B_2^{\circ}[f]+C^{\circ}[f]+C_{pd}^{\circ}[f]) + {}^{\circ}C[b]$ ${}^{\circ}C[b] = - \min\{ C_{kb}.f([w]).C^{\circ}[b], {}_{ox}^*\}$ | mmol C m ⁻² d ⁻¹ |
| ... nitrogen, $M^{\circ}[b]$ | $dM^{\circ}[b]/dt = k_f.(N_1^{\circ}[f]+N_2^{\circ}[f]+M^{\circ}[f]+M_{pd}^{\circ}[f]) + {}^{\circ}M[b]$ ${}^{\circ}M[b] = - {}^{\circ}C[b].MQ[b]$ | mmol N m ⁻² d ⁻¹ |
| ... silica, $SiM^{\circ}[b]$ | $dSiM^{\circ}[b]/dt = k_f.(SiN_1^{\circ}[f]+SiM^{\circ}[f]+SiM_{pd}^{\circ}[f]) + {}^{\circ}SiM[b]$ ${}^{\circ}SiM[b] = - Si_{kb}.f([w]).SiM^{\circ}[b]$ | mmol Si m ⁻² d ⁻¹ |

See text concerning details for fluff and water layers.

(b) parameters

| Symbol | Parameter | Value | Units |
|----------------|---|--------|--|
| A_1 | Initial fluff amount of fine inorganic sediment | 30.0 | g m ⁻² |
| w_{A1} | Sinking rate of fine iSPM | -5.0 | m d ⁻¹ |
| σ_0 | reference bed stress | 0.1 | kg m ⁻¹ s ⁻¹ |
| n | exponent of resuspension equation | 3 | |
| s | fluff resuspension coefficient | 0.0020 | g m ⁻² s ⁻¹ |
| k_f | fluff to sediment bioturbation rate (at 20°C) | 0.3 | d ⁻¹ |
| k_d | rate at which microplankton in fluff decays to detritus (at 20°C) | 0.1 | d ⁻¹ |
| Si_{k_f} | decay rate of fluff biogenic silica (at 20°C) | 0.1 | d ⁻¹ |
| C_{kb} | decay rate of labile sediment organic carbon (at 20°C) | 0.02 | d ⁻¹ |
| Si_{kb} | decay rate of sediment biogenic silica (at 20°C) | 0.04 | d ⁻¹ |
| E | sediment-water exchange velocity (at 20°C) | 0.01 | m d ⁻¹ |
| h_b | thickness of sediment, | 0.05 | m |
| O_{min} | minimum sediment pore water oxygen | 3 | mmol O ₂ m ⁻³ |
| $NO_{S_{min}}$ | minimum sediment pore water nitrate | 0.1 | mmol N m ⁻³ |
| NO_{q^C} | nitrate required to oxidize organic carbon during denitrification | 0.8 | mmol NO ₃ ⁻ (mmol C) ⁻¹ |

Appendix: Aggregation

Jackson (2001) applied a coagulation scheme with up to 30 size-classes to the biological model of Fasham *et al.* (1990), giving sinking speeds from 0.002 to 558 m d⁻¹. In contrast, the sinking rate spectrum in 2MPPD is discretised into only four compartments, although the speed range covers 0 to 100 m d⁻¹.

2MPPD compartments in relation to aggregation and sinking

| compartments | defined radius, µm | speed of sinking under gravity, m d ⁻¹ | aggregation and similar changes of state |
|---------------------------------|--------------------|---|---|
| MP2 (flagellatey microplankton) | 1.5 | 0.0 | grazing-defecation converts to detritus |
| MP1 (diatomy microplankton) | 5.0 | 0.5 - 5.0 | aggregate to form phytodetritus; grazing-defecation converts to detritus |
| detritus | not defined | 5 | formed by grazing, and by decay of others in fluff layer, but don't aggregate |
| phytodetritus | not defined | 100 | formed from MP1 by aggregation; decays to detritus in fluff layer |

In the main part of 2MPPD, the defined cell radii influence rates that depend on surface-volume ratios; here we use them to influence aggregation, introducing a minimum of extra parameters. The main task of our aggregation formulation is to drive a process that may truncate the Spring bloom and rapidly convert high concentrations of euphotic layer microplankton into remineralisable material in the fluff layer. The physical process of coagulation is deemed to occur only between cells of diatomy microplankton, and results in the formation of rapidly sinking phytodetritus. No other particle classes are involved, although the microheterotrophs that are part of MP1 are assumed to take part along with the diatoms. Simulated grazing and defecation converts non-sinking MP2, as well as MP1, into detritus, which provides a slower route to the fluff layer. The decay of phytodetritus to detritus to some extent simulates disaggregation.

2MPPD deals in bulk concentrations. However, we begin by considering encounters between cells of MP1, assumed to be possessed of the mean properties of included microplankters. In principle, coagulation can result from Brownian motion, shear-driven collision, or differences in sinking speed. We consider only collisions resulting from relative movement of identical cells due to shear, a process parameterized by the collision kernel

$$(a1) \quad b_a = (1.3) \cdot s \cdot (r_e + r_e)^3 \quad m^3 s^{-1}$$

(Pruppacher & Klett, 1980; Jackson, 1990). This kernel might be said to give the volume swept by the trajectory of a single cell during a second. The extent of sweeping is defined by the cell's encounter radius, r_e , and movement relative to other cells by the shear, s .

Shear arises from two causes. One is the viscously damped effect of turbulent eddies over distances less than the Taylor microscale, which is of order centimetres according to the physical model. This micro-shear can be calculated from turbulent kinetic energy dissipation rate ($\text{m}^2 \text{s}^{-3}$) in the physical model:

$$(a2) \quad s = (\epsilon / \nu)^{0.5} \quad \text{s}^{-1}$$

where ν is molecular viscosity ($\text{m}^2 \text{s}^{-1}$). In addition, there are larger-scale gradients of velocity:

$$(a3) \quad s = ((v_x/z)^2 + (v_y/z)^2)^{0.5} \quad \text{s}^{-1}$$

where v_x and v_y are velocity components provided by the physical model with resolution of z . Figure A1(a) shows profiles of shear on day 122 of simulation NW03. Except in the upper thermocline, micro-shear (eqn. a2) is bigger than macro-shear (eqn. a3).

Returning to eqn. (a1), the collision kernel can be used to calculate a volume encounter rate per cell, the product $b_a \cdot n$ where n is the MP1 cell concentration. It is the probability that the one-second trajectory volume of a given cell will overlap the trajectory volume of another, similar, cell. The parameter a_s , stickiness, gives the proportion of these encounters that result in aggregation. Thus the cell loss rate due to aggregation, is

$$(a4) \quad \text{relative loss rate} = 2 \cdot a_s \cdot b_a \cdot n \quad \text{s}^{-1}$$

The factor 2 appears because each sticky encounter results in the loss of two cells.

Equations (a1) and (a4) relate to single cells. A bulk rate can be calculated by applying the cell loss rate in (a4) to the bulk microplankton biomass B_1 , giving the daily loss flux due to aggregation as:

$$(a5) \quad \text{agg}B1 = -2 \cdot a_s \cdot b_a \cdot n \cdot B_1 \cdot (86400) \quad \text{mmol C m}^{-3} \text{ d}^{-1}$$

Cell concentration in this hybrid equation is estimated by $n = B_1 / C_q^n$. C_q^n is the carbon biomass content of a spherical cell, given by:

$$(a6) \quad C_q^n = (4/3 \cdot \pi \cdot r_m^3) \cdot C_q^v \quad \text{mol C cell}^{-1}$$

where C_q^v is the typical content of organic carbon per unit volume of diatomey microplankter protoplasm, taken as $1 \times 10^4 \text{ mol m}^{-3}$. The radius of mass r_m of diatomey microplankton is defined as $5 \mu\text{m}$, and hence $C_q^n = 5.24 \text{ pmol C cell}^{-1}$.

Combining the geometric and numerical constants from (a5) in a single factor gives the form used in the main text

$$(a7) \quad \text{agg}B1 = k_a \cdot a_s \cdot s \cdot B_1^2 \quad \text{mmol m}^{-3} \text{ d}^{-1}$$

where

$$k_a = (86400).(1.3).(2.r_e)^3/((4/3).r_m^3).C_{qv} = (0.0215).(r_e^3/r_m^3) \text{ m}^3 (\text{mmol C})^{-1} \text{ s d}^{-1}$$

The radius terms cancel if a cell's encounter radius is the same as the radius defining its volume and biomass. This might not be the case; a spiny diatom might well have an encounter radius that is larger than the radius of the sphere equal to the cell's protoplasmic volume. Thus we define the correction factor r^* as the cube of the ratio of the encounter and mass radii, and hence

$$(a8) \quad k_a = (0.0215).r^* \text{ m}^3 (\text{mmol C})^{-1} \text{ s d}^{-1}$$

The factor is equivalent to r_e^{3-D} , where D is the fractal dimension that specifies the relationship between a particle's apparent volume and its volume when converted to a solid sphere (Jackson *et al.*, 1997).

In the main text we explored the effect of $r^* = 1$ (all NC and most NW simulations) and $r^* = 10$ (NW04), as well as the effect of changing stickiness from 0.25 to 1.0, using shear calculated by eqn. (a2).. Figure A1(b)* gives values of relative bulk loss rate due to aggregation, calculated from

$$(a9) \quad \text{loss rate} = k_a.a_s.s.B_1 \text{ d}^{-1}$$

Rates are shown for several scenarios, with different values of the aggregation parameters and biomass. The low value of diatomey microplankton biomass B_1 equates with about 1 mg chlorophyll m^{-3} , the high biomass with about 5 mg m^{-3} , close to the peak of the Spring bloom in NW03. Rates at different levels of shear, corresponding to different parts of the water-column and different ways of calculating shear, may be compared with typical growth rates of diatomey microplankton, which reached 0.4 d^{-1} during the Spring bloom, and more generally span an order of magnitude around 10^{-1} d^{-1} . It can be seen that significant aggregation loss occurs only in parts of the water-column where shear is high, and that the larger values of a_s and k_a are likely to lead to excessive losses when aggregation is driven by micro-shear (as was standard in simulations reported in the main text).

* Figure A1. (a) profiles of micro-shear (eqn. a2) and macro-shear (eqn. a3) in simulation NW03 on day 122. (b) Relative aggregation loss rate according to eqn. a9, for four scenarios representing different values of the aggregation parameters k_a and a_s and diatomey microplankton biomass B_1 . The low values of the aggregation parameters are the standard values, $k_a = 0.0215 \text{ m}^3 (\text{mmol C})^{-1} \text{ s d}^{-1}$ and stickiness $a_s = 0.25$. The high values are: $k_a = 0.215 \text{ m}^3 (\text{mmol C})^{-1} \text{ s d}^{-1}$ and $a_s = 1.0$. The low value (3 mmol C m^{-3}) of diatomey microplankton biomass B_1 equates with about 1 mg chlorophyll m^{-3} , the high biomass with about 5 mg m^{-3} . The shaded region shows aggregation loss rates that are of the same order of magnitude as microplankton growth rates and other main loss rates.

